

Supporting information

The “jump of size” phenomenon in aqueous-nanoparticle reaction system : phase transformation from nano-Mg(OH)₂ to bulk MgCO₃·3H₂O--

5

Supplementary Material

YongJing Wang^a, Weizhen Liu^a, Feng Huang^b, Ting Zou^a, Zhang Lin^{a,*}

^aState Key Laboratory of Structural Chemistry, Fujian Institute of Research on the Structure of Matter, Chinese Academy of Sciences, Fuzhou, Fujian, 350002, China

^bKey Laboratory of Optoelectronic Materials Chemistry and Physics, Fujian Institute of Research on the Structure of Matter, Chinese Academy of Sciences, Fuzhou, Fujian, 350002, China

*Corresponding author: zlin@fjirsm.ac.cn,

1. Experimental Section:

1.1 Materials and Instruments.

15 All of the chemicals were AR reagents obtained from commercial sources and used without further purification.

X-ray diffraction (XRD) was used to identify phase and crystal structure of the obtained samples. Diffraction data were recorded using a PANalytical X' Pert PRO diffractometer with Cu K α radiation (40 kV, 40 mA) in the continuous scanning mode. The 2 θ scanning range was from 10° to 80° in step 20 of 0.03° with a collection time of 20 s per step. Scanning electronic microscopy (SEM) analyses were used to confirm the particle sizes and to determine the particle morphology. Samples were prepared for SEM study by dispersing the ZnS powder onto a holey carbon-coated support. The SEM analyses were performed using a JSM-6700F equipped with an Oxford-INCA energy dispersive X-ray (EDX) spectroscopy. Samples were prepared for TEM study by dispersing the powder onto 200-mesh carbon-coated copper grids. TEM analyses were performed using a JEOL JEM2010 HRTEM instrument at 200 kV.

1.2 Synthesis of Mg(OH)₂ lamellas.

Mg(OH)₂ nano-lamellas could be prepared by putting MgO into low concentration NaNO₃ solutions. The typical condition for batch experiment was: heating 20 g of MgO at 600 °C for 2 h, then 30 quenching the powder in 5 L NaNO₃ solutions (1× 10⁻⁴ M). The mixture was stirred for 24 h, until the

MgO was totally transformed to Mg(OH)₂. Then it was filtered out and washed with deionized water for three times. The sample was air dried for XRD and SEM analyses, and the for the carbonation experiments.

1.3 control experiments for the carbonation of Mg(OH)₂ lamellas.

5 Above Mg(OH)₂ was mixed with about 50 mLH₂O. The mixture were transferred into a cylindrical stainless steel vessel directly, and then stirred into slurry-like mixture. The stainless steel vessel was then sealed and filled with CO₂ at 0.3 MPa for 6 h, and 0.1 Mpa for 12h respectively. At different time interval, a small amount of the solid product was collected for XRD analysis, TEM, and SEM observation.

10 1.4 Synthesis of MgCO₃•3H₂O via nucleation and growth method

The Na₂CO₃ (0.1 M) was dropped into MgCl₂ (0.1 M) directly, and the mixture were stirred at 303 K for 5 min. The resulting white precipitate was collected for XRD analysis, TEM, and SEM observation.

1.5 Cr^{VI} desorption of the Cr-adsorbed nano-Mg(OH)₂.

15 The Cr-adsorbed nano-Mg(OH)₂ was obtained by putting MgO into simulated Cr^{VI}-containing wastewater. The typical condition was: heating 20 g of MgO at 600 °C for 2 h, then quenching the powder in 5 L simulated Cr^{VI}-containing (5 mg·ml⁻¹) wastewater immediately. The saturated adsorption capability (Q_e) of Mg(OH)₂ to Cr^{VI} is 0.82 mg·g⁻¹.

Cr^{VI} -adsorbed Mg(OH)₂ that containing with about 50 mL solution was transferred into a cylindrical
20 stainless steel vessel, and then stirred into slurry-like mixture. The stainless steel vessel was then sealed and filled with CO₂ at 0.3 MPa for 6 h. After carbonation treatment, the mixture could be separated clearly into yellow concentrated solution of Cr^{VI} and yellowish MgCO₃•3H₂O precipitate. At different time intervals, the solution of Cr^{VI} was separated for Cr^{VI} determination.

2. Results

25 2.1 The characterization of the as-synthesized MgCO₃•3H₂O which was obtained via nucleation and growth method

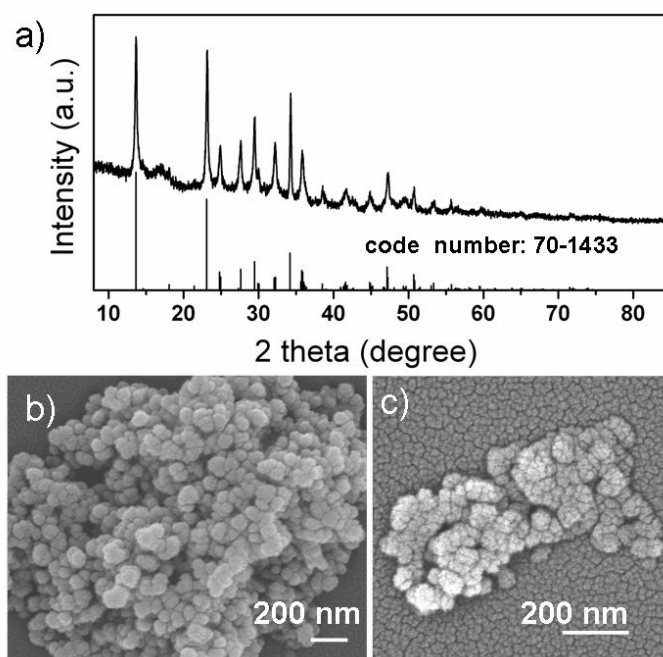


Figure S1. The XRD pattern (a) and SEM images (b, c) of the $\text{MgCO}_3 \cdot 3\text{H}_2\text{O}$ which is obtained by direct mixing of MgCl_2 (0.1 M) and Na_2CO_3 (0.1 M) at 303 K.

5.2.2 A detail time series XRD analysis for the carbonation process in which the $\text{MgCO}_3 \cdot 3\text{H}_2\text{O}$ phase began to emerge.

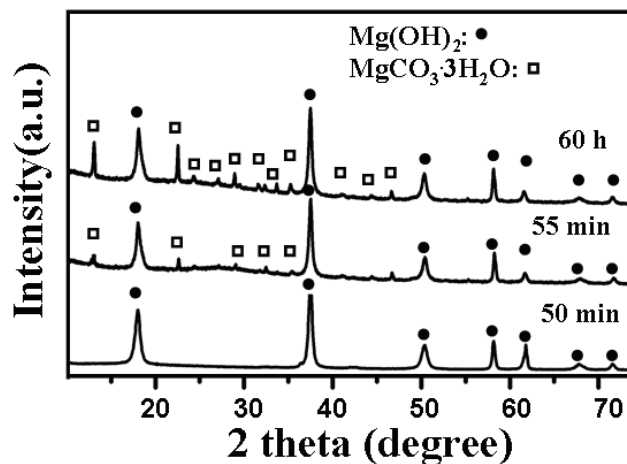


Figure S2. Time series XRD analysis of the samples carbonated by CO_2 with pressure of 0.3 Mpa at room temperature

10

2.3 The profile analysis of the XRD data.

All peak profiles have been seriously decomposed in elementary curves. Fig. S3 shows the profile analysis of XRD data of the product after 1 h 45 min carbonation.

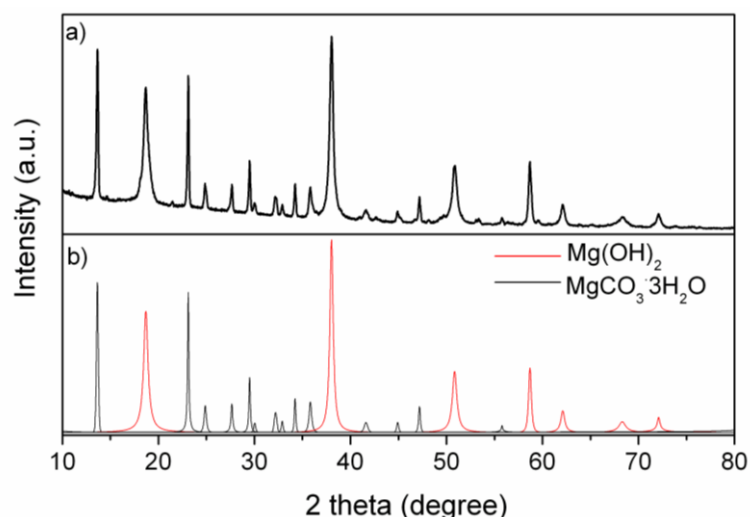
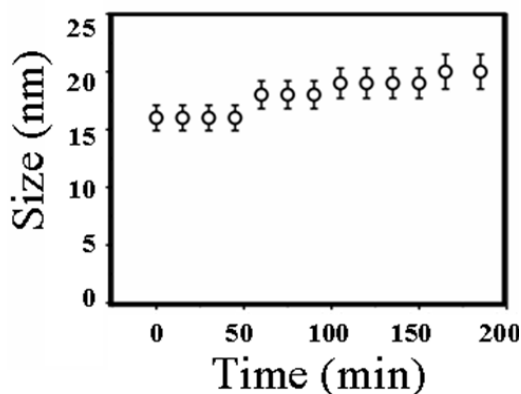


Figure S3. a) The raw data of the XRD pattern of the product after 1 h 45 min carbonation. b) Profile analysis of the XRD pattern shown in a which has been decomposed in elementary peaks

2.4 The size evolution of Mg(OH)₂ during the carbonation process.



5

Figure S4 The size evolution of Mg(OH)₂ during the carbonation process.

2.5 Supplementary SEM image for Fig. 3b.

It shows in XRD diagram (Fig. 2 in the text) that the main phase is Mg(OH)₂ after one hour 10 carbonation. A small amount MgCO₃·3H₂O could also be detected by XRD, indicating the formation of the MgCO₃·3H₂O. Fig3b shows the SEM morphology of the main phase after one hour carbonation. As indicated by the XRD pattern, the main phase at the time is Mg(OH)₂. Thus, large amount of lamellas were observed in SEM. Actually, except the Mg(OH)₂ lamellas, sporadic rod-like MgCO₃·3H₂O could also be observed, as shown in **Fig. S5**.

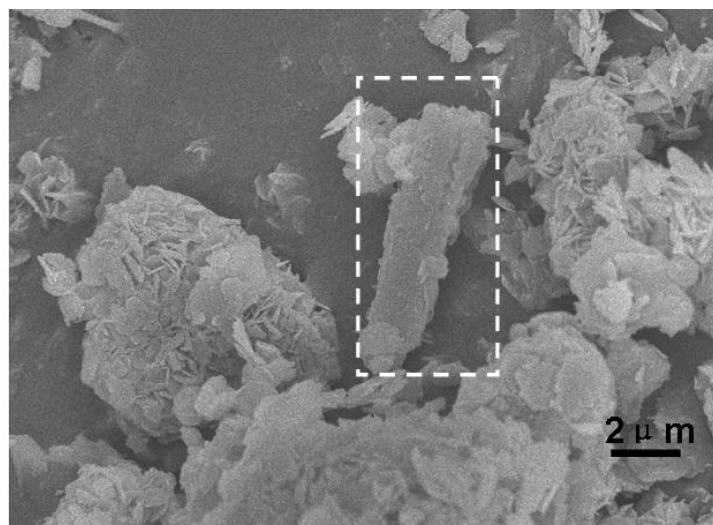


Figure S5. The SEM image of the carbonation product with pressure of 0.3 MPa at room temperature for 1 h. The area in white dotted box shows a rod-like particle with the size up to ~ 10 μm.

5 2.6 Crystal face indexation for $\text{MgCO}_3 \cdot 3\text{H}_2\text{O}$

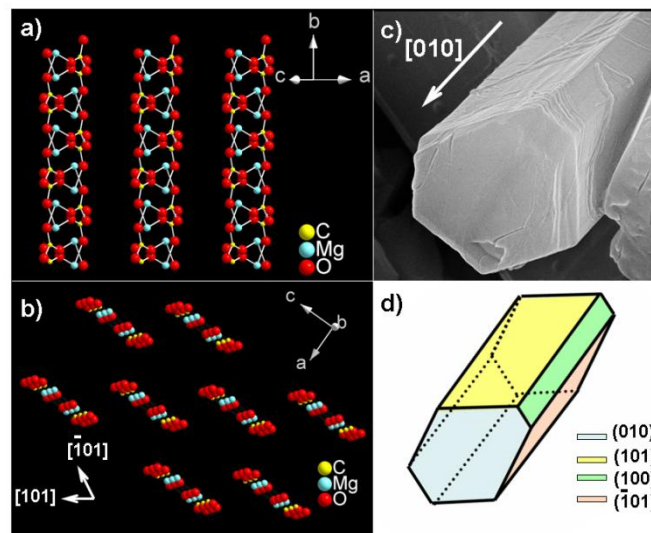


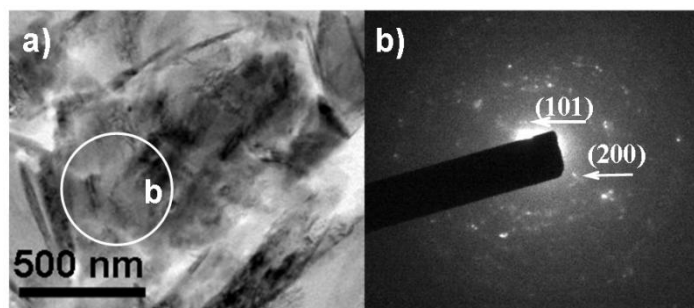
Figure S6. The phase structures of $\text{MgCO}_3 \cdot 3\text{H}_2\text{O}$ projected along [101] (a) and [010] directions (b) respectively. The inter-ribbon water molecules are deleted for clarity. c) The SEM of a typical single crystal of $\text{MgCO}_3 \cdot 3\text{H}_2\text{O}$ d) a sketch of the single crystal shown in c) with every face indexed.

10

2.7 The SEAD pattern for a typical crystal-like micro-rod covered with lamellas

Fig. S5 shows that only weak (101) and (200) reflection of $\text{MgCO}_3 \cdot 3\text{H}_2\text{O}$ could be observed. We also observed reflections that could not be assigned to that of $\text{MgCO}_3 \cdot 3\text{H}_2\text{O}$, indicating that $\text{MgCO}_3 \cdot 3\text{H}_2\text{O}$ has decomposed after the electron beam irradiation. But no reflection of $\text{Mg}(\text{OH})_2$ was observed. Since

XRD patterns indicates that there only two phase during the whole phase transformation, it could be infer that the phase shown in Fig. S5a (the domain inside the while circle) is $\text{MgCO}_3 \cdot 3\text{H}_2\text{O}$.



5 **Figure S7** a) a typical TEM image of the specimen cut form the crystal-like micro-rods covered with lamellas, b) SEAD pattern of sample shown a

2.8 The carbonation process on the condition that the P_{CO_2} is 0.1 MPa.

When the pressure of CO_2 is relatively low, it will take more time (12h) for the transformation from 10 $\text{Mg}(\text{OH})_2$ to $\text{MgCO}_3 \cdot 3\text{H}_2\text{O}$. And artinite $\text{Mg}_5(\text{CO}_3)_3(\text{OH})_2 \cdot 3\text{H}_2\text{O}$ would appeared as a metastable species, as shown in **Fig. S6**.

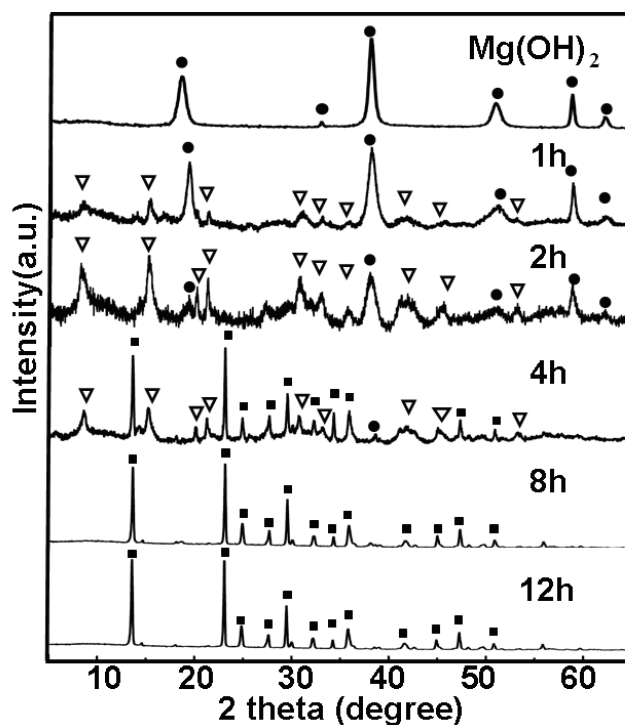


Figure S8. Time series XRD analysis of the samples carbonated by CO_2 with pressure of 0.1 MPa at room temperature (● $\text{Mg}(\text{OH})_2$, ▽ $\text{Mg}_5(\text{CO}_3)_4(\text{OH})_2 \cdot 3\text{H}_2\text{O}$, ■ $\text{MgCO}_3 \cdot 3\text{H}_2\text{O}$)

15 2.9 Cr^{VI} desorption of the Cr-adsorbed nano- $\text{Mg}(\text{OH})_2$.

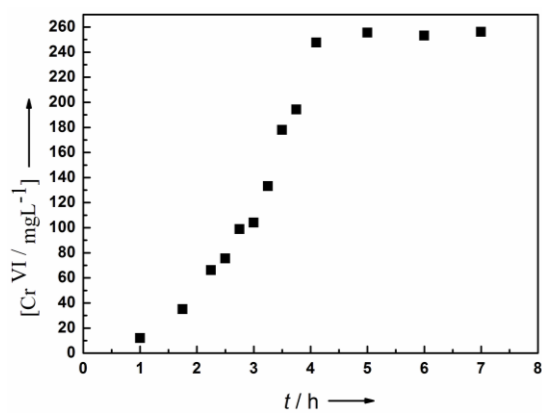


Figure S9. The Cr^{VI} concentration in the supernatant during carbonation treatment of Cr^{VI} -loaded $\text{Mg}(\text{OH})_2$ ($Q_e = 0.82 \text{ mg/g}$).